Pure & Appl. Chem., Vol. 57, No. 2, pp. 355–367, 1985.
Printed in Great Britain.

Transport properties of electrolytes from infinite dilution to saturation

J. Barthel

Institut für Physikalische und Theoretische Chemie der Universität Regensburg, D-8400 Regensburg, Germany.

Abstract - Temperature and concentration dependence both of electrolyte conductances and transference numbers are discussed for various electrolyte solutions. The properties of the solvents and the ionic friction coefficients are correlated with solvent viscosities, permittivities and relaxation times. The permittivities and relaxation times of the solutions are studied as a function of frequency and electrolyte concentration.

For dilute solutions consistent and reliable equations are based on the chemical model which takes into account short and long-range forces within the framework of the McMillan-Mayer-Friedman theories. The treatment of concentrated solutions uses the model of cooperatively rearranging domains and rationalizes the effects due to ion-ion and ion-solvent interactions in terms of the parameters characterizing the behaviour of electrolytes in dilute solution.

1. INTRODUCTION

For a long period non-aqueous electrolyte solutions stimulated the interest of scientists only in fundamental research. Solvents and solvent mixtures yield ideal model media for the study of ion-ion interactions in dielectrics of permittivities ranging from 2 to 200.

Nowadays non-aqueous electrolyte solutions are intensively studied for tackling technical problems owing to their wide spread of physical properties such as viscosity, permittivity, freezing and boiling point or vapour pressure. Large liquid ranges, wide cathodic and anodic stability ranges, large ranges of acid-base properties, good solubility properties for various compounds - electrolytes as well as non-electrolytes - high stability of the solutions and compatibility with cathode materials permit the formulation of numerous electrolyte solutions possessing attributes planned on the drawing board by the engineer (1,2).

Various attempts have been made to classify solvents according to selected physical properties or empirical interaction parameters (3). In spite of all its limitations such a classification of solvents into classes is useful for rationalizing the choice of appropriate solvents and solvent mixtures for particular investigations.

Present-day techniques permit highly precise measurements from very low electrolyte concentrations to saturation over large temperature ranges. This paper attempts to provide some understanding of the transport properties of electrolyte solutions, especially their temperature dependences in various solvents, based on experimental data.

2. ELECTROLYTES AT LOW CONCENTRATIONS

There is no doubt that the Debye-Hückel limiting laws can be confirmed by highly precise measurements at low concentrations both for transport and thermodynamic properties, even in solvents of moderate permittivity. Well-founded extrapolation methods are needed for the estimation of limiting values from the measurements at low concentrations where the competition of solvent structure and ion-solvent interactions is not negligible (2).

The McMillan-Mayer-Friedman (MMF)-level Hamiltonian models provide the appropriate basis for the treatment of electrolyte solutions at low concentrations. Such models use pairwise additive potential functions of the solvent-averaged forces between the ions for calculations of the solution properties (4). The chemical model, including short and long range forces, (2,5-7) has proved to be successful for every electrolyte solution so far investigated in our laboratory. According to Friedman "success would mean that we can understand all of the observations in terms of solvent-averaged forces between the ions" (4).

Properties of electrolyte solutions, E(c;p,T), at low concentrations c can be represented by a set of equations (7)

$$E(c;p,T) = E^{\infty}(p,T) + E'(\alpha c;p,T;R,W_{ij}); \quad \frac{1-\alpha}{\alpha^2 c} = K_c(c;p,T;R,W_{ij}) \qquad (1a,b)$$

where $E^{\infty}(p,T)$ is the limiting value of the property E(c;p,T) at zero concentration and K_c is the so-called association constant in the molarity scale.

2.1 The chemical model

At the lowest approximation level the chemical model subdivides the space around an ion into three regions (5,7)

i) $r < a$, a being the minimum distance of two ions, i and j, which is assumed to be the sum of the effective ion radii, $a = a_i + a_j$.

ii) $a \leq r \leq R$, the range of short range interactions. For dilute solutions with high to moderate permittivities this region is generally occupied only by paired states of oppositely charged ions.

iii) $r \geq R$, the region of long range interactions.

For other approximations see ref. (2).

The mean force potentials of regions (ii) and (iii), $W_{ij}^{(I)}$ and $W_{ij}^{(II)}$, are split into two parts representing coulombic, $W_{ij}^{(I)}$, and non-coulombic, W_{ij}^{*}, interactions

$$W_{ij}^{(\alpha)} = W_{ij}^{el(\alpha)} + W_{ij}^{*(\alpha)}, \quad \alpha = \text{I or II} \qquad (2)$$

Region (i) is characterized by a hard core potential. The link between the chemical model and the experimentally determined property of the solution - with the exception of scattering experiments which yield the pair correlation functions, g_{ij}, via structure factors - is an integral expression of type

$$\int r^2 (g_{ij} - 1)dr = \int_a^R r^2(g_{ij}^{(I)} - 1)dr + \int_R^{\infty} r^2(g_{ij}^{(II)} - 1)dr; \quad g_{ij}^{(\alpha)} = \exp\left[-\frac{W_{ij}^{(\alpha)}}{kT}\right] \qquad (3)$$

The ion-association concept for symmetrical electrolytes can be easily introduced into the model, assuming that the distance parameter R equals the upper limit of ion association. The relationship (5)

$$W_{+-}^{(I)} = -\frac{2qkT}{r} + \frac{2q\kappa kT}{1+\kappa R} + W_{+-}^{*} \qquad (4)$$

where

$$\kappa^2 = 16\pi N_A q\alpha(10^3 c); \quad q = \frac{e_o^2 z^2}{8\pi\varepsilon_o \varepsilon kT} \qquad (5a,b)$$

yields the integral (a ... R) of eq. (3) in the form

$$\int_a^R r^2 \exp\left[-\frac{W_{ij}^{(I)}}{kT}\right]dr = \exp\left[-\frac{2q\kappa}{1+\kappa R}\right] \int_a^R r^2 \exp\left[\frac{2q}{r} - \frac{W_{+-}^{*}}{kT}\right]dr \qquad (6)$$

In eqs. (5) ε is the relative permittivity of the solvent, ε_o is the permittivity of the vacuum, e_o is the charge of proton, k is the Boltzmann constant, N_A is the Avogadro number, T is the temperature, and α is the fraction of the ions with mutual separations greater than R(r > R, 'free' ions). All quantities require SI units except concentration c which is used in the molarity scale, mol dm^{-3}. Eq. (6) is linked to the ion-pair association constant, K_A, and the mean activity coefficient of the free ions, $y_{\pm}'$, by the relationships

$$\frac{1-\alpha}{\alpha^2 c}\frac{1}{y_{\pm}'^2} = K_A = 4\pi N_A \times 10^3 \int_a^R r^2 \exp\left[\frac{2q}{r} - \frac{W_{+-}^{*}}{kT}\right]dr; \quad y_{\pm}' = \exp\left[-\frac{\kappa q}{1+\kappa R}\right] \qquad (7a,b)$$

The distance parameter can either be determined by experiments or be set by chemical evidence. A comprehensive investigation of solution properties in various solvents with a multitude of electrolytes shows that R corresponds to the sum of distances of closest ion approach, a in the region (i), and the dimension of one or more orientated solvent molecules (2,7).

2.2 Electrolyte conductances and transference numbers

Both electrolyte conductances and transference numbers are required for a proper understanding of charge transport by ions in electrolyte solutions. In spite of a steady growth of interest in the pressure and temperature dependence of transport properties of non-aqueous electrolyte solutions only scarce information is available in this field.

Concerning the state of theory of transference numbers and ion conductances the reader is referred to Spiro's survey (8) and the contributions of Justice, Perić, and Perić (9,10). Temperature dependence is discussed in recent papers from our laboratory (11,12). Krumgalz (13)

quotes and analyses 17 empirical methods to replace the experimentally difficult and time-consuming measurements of transference numbers by methods based on empirical assumptions, such as splitting electrolyte conductance into ionic contributions or calculating ion conductances in one solvent from those in another by the help of Walden's rule.

The literature on conductance is quoted in refs. (2,6); a survey of temperature dependence data is given in ref. (14). The state of conductance theory was recently surveyed by Justice (15). Altenberger and Friedman (16) present a new statistical-mechanical theory of isothermal transport coefficients, and Pethybridge (17) reports on non-symmetrical electrolytes.

Conductance measurements on dilute solutions of symmetrical electrolytes are reproduced by equations of type

$$\Lambda = \Lambda^{\infty} - \Lambda^{r} - \Lambda^{e} \tag{8a}$$

$$\text{or } \frac{\Lambda}{\alpha} = \Lambda^{\infty} - S(\alpha c)^{1/2} + E\alpha c \log(\alpha c) + J_1(R)\alpha c - J_2(R)(\alpha c)^{3/2} \tag{8b}$$

Eq. (8b) is a truncated series development of the general equation (8a) where Λ^{∞} is the limiting electrolyte conductance; Λ^{r} and Λ^{e} are the contributions from the relaxation and electrophoretic effects at electrolyte concentration c[mol dm^{-3}]. Sets of coefficients in eq. (8b) are given in refs. (18,19). Distance parameters R are chosen in agreement with the chemical model, supposing that only the free ions ($r > R$) contribute to electrolyte conductance. Data analysis is based on the set of equations (1) where eq. (1a) is replaced by eq. (8b).

Single ion conductances contain electrophoretic, λ^{e}, and relaxation contributions, $\Delta X/X$, yielding eq. (9a). Neglecting the contribution which is due to the space-dependent part of the interionic two particle force allows us to write λ^{e} in the form of eq. (9b), see ref. (10).

$$\lambda_i = \lambda^{e} + \lambda_i^{\infty}\left(1 + \frac{\Delta X}{X}\right); \quad \lambda^{e} = 0.5\,\Lambda^{e}\left(1 + \frac{\Delta X}{X}\right) \tag{9a,b}$$

Transference numbers of 1,1-electrolytes are related to the single ion conductances λ_i and the electrolyte conductance, $\Lambda = \lambda_+ + \lambda_-$, by eqs. (10a,b). The combination of eqs. (9a,b) and (10a,b) leads to the commonly applied relationship (10c) (8,10,11,20,21).

$$t_i = \frac{\lambda_i}{\Lambda}; \quad t_i^{\infty} = \frac{\lambda_i^{\infty}}{\Lambda^{\infty}}; \quad \frac{t_i - 0.5}{t_i^{\infty} - 0.5} = \frac{\Lambda^{\infty}}{\Lambda^{\infty} + \Lambda^{e}} \tag{10a,b,c}$$

For the truncated series development of Λ^{e} in terms of the coefficients of the conductance equation, see ref. (8,10,11). Data analysis is based on eqs. (1) with eq. (10c) as the eq. (1a).

2.3 Temperature-dependence of transference numbers

Recent developments have rendered temperature-dependent transference numbers accessible to measurement. Two types of families of curves are found in agreement with the theory (11). Electrolyte solutions showing $t_+^{\infty} < 0.5$ yield functions $t_+ = t_+(c,T)$ decreasing with increasing concentration and decreasing temperature in contrast to those with $t_+^{\infty} > 0.5$, see Fig. 1. Further examples for the first class are KCNS solutions in ethanol and propanol and Me_4NClO_4 and Et_4NClO_4 solutions in acetonitrile (11).

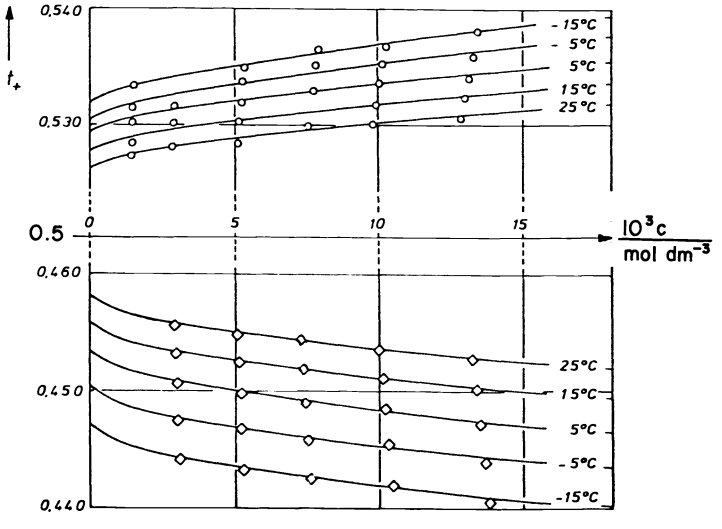

Fig. 1. Temperature- and concentration-dependence of methanol solutions of Me_4NCNS (o) and KCNS (◇).

Krumgalz (13) has stressed the fact that Walden's rule for estimating single ion conductances λ_i^∞ by correlations of transference numbers with viscosities in different solvent media does not yield reliable data. Reasonably approximated data are obtained, however, for estimates of the temperature dependence of single ion conductances in a solvent with the help of the relationship

$$\lambda_i^\infty(T_1)\eta(T_1) = \lambda_i^\infty(T_2)\eta(T_2) \qquad (11)$$

Table 1 compares the limiting values $\lambda_-^\infty(ClO_4^-/AN)$ and $\lambda_-^\infty(CNS^-/MeOH)$ each one determined from two independent measurements of transference numbers t_+^∞ with the values obtained by application of eq. (11); the reference temperature is 25°C. The maximum differences of about 1 % in acetonitrile and 3 % in methanol characterize the approximations of eq. (11) in an aprotic and a protic solvent, respectively.

TABLE 1. Limiting ion conductances at various temperatures from transference numbers and Walden's rule.

Temp.	$\lambda_-^\infty(ClO_4^-)$ in acetonitrile from			$\lambda_-^\infty(CNS^-)$ in methanol from		
$\frac{\Theta}{^oC}$	$t_+^\infty(Et_4NClO_4)$ eq. (10b)	$t_+^\infty(Me_4NClO_4)$ eq. (10b)	W.R. eq.(11)	$t_+^\infty(Me_4NCNS)$ eq. (10b)	$t_+^\infty(KCNS)$ eq.(10b)	W.R. eq.(11)
+25	103.57	103.72	(103.65)	61.87	61.95	(61.91)
+15	94.13	94.24	94.05	53.93	53.97	53.57
+ 5	84.91	85.01	84.65	46.57	46.60	45.92
- 5	75.94	76.00	75.48	39.84	39.82	38.94
-15	67.20	67.25	66.58	33.64	33.61	32.63
-25	58.72	58.75	58.00			
-35	50.54	50.58	49.93			

No pronounced differences are observed for the temperature coefficients of single ion conductances in a given solvent. Ethanol solutions at 25°C exhibit values of $d\ln \lambda_i^\infty/d(1/T)$ in a small interval around -1.64×10^3 K for all cations and anions (12). This feature will find an explanation by the model of cooperatively rearranging domains.

Variation of the Walden product and its temperature coefficient is discussed in the literature in terms of structure making and structure breaking effects; for quotations see ref. (14).

The small variation of transference numbers, cf. Fig. 1, does not permit their use for determining distance parameters R or association constants K_A. These quantities must be obtained by other methods for the use in the data analysis of transference number measurements.

2.4 Information from permittivity measurements

Investigations of the high frequency permittivities of electrolyte solutions provide important dielectric data, especially since precise measurements at electrolyte concentrations from 10^{-3} M to saturation are possible. The schematic representation of two types of Argand diagrams, Fig. 2, obtained from these measurements demonstrates the notions needed for the further discussion. The quantities $\varepsilon'(\nu)$ and $\varepsilon''(\nu)$ are the real and imaginary parts of the complex permittivity, $\varepsilon(\nu) = \varepsilon'(\nu) - j\,\varepsilon''(\nu)$, depending on the frequency ν of the electromagnetic wave applied and on concentration and temperature of the solution.

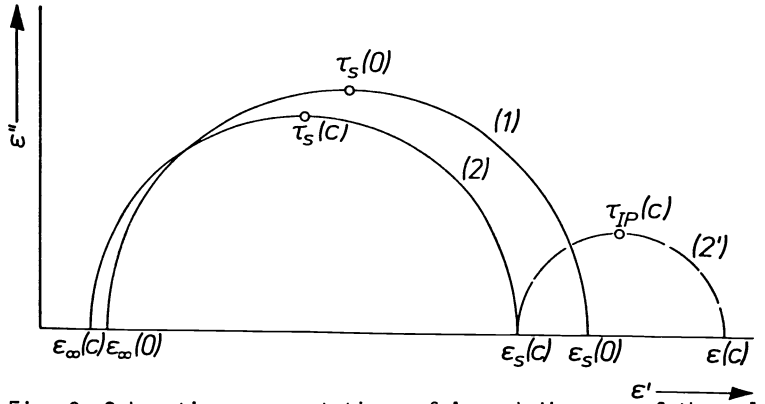

Fig. 2. Schematic representations of Argand diagrams of the solvent (1) and electrolyte solutions (2) and (2 + 2').

The semicircle (1) is obtained for the pure solvent, the intersections on the ε'-axis are the static permittivity $\varepsilon(0)$ and the high frequency permittivity $\varepsilon_\infty(0)$. Addition of the electrolyte shifts $\varepsilon_S(0)$ to $\varepsilon_S(c)$ and $\varepsilon_\infty(0)$ to $\varepsilon_\infty(c)$, yielding the relaxation curve (2) of the solvent at electrolyte concentration c. An additional relaxation region represented by the broken line (2') is attributed to the relaxation of ion pairs, but is only observed under appropriate stability conditions. The ion-pair relaxation region exists for 2,2-electrolytes in aqueous solutions (19,22), 1,1-electrolytes in low permittivity solvents (23,29), and may also exist for some non-symmetrical electrolytes in high permittivity solvents, e.g. $ZnBr_2$ in propylene carbonate (25). Ion pairs of 1,1-electrolytes in solvents of high or moderate permittivities do not exhibit relaxation (2,24). Hence two general types of Argand diagrams can be found for electrolyte solutions, type (2) or type (2 + 2'). The frequency at the apex of each semicircle is the reciprocal relaxation time τ of the corresponding relaxation process. Suffice it to note that the real Argand diagrams are more complex. Depending on molecular symmetries and the possibility of cooperative movements, even pure solvents exhibit more than a single relaxation time; every relaxation time identified is the center of gravity of a more-or-less broad relaxation time distribution.

Recent theories (26-28) link the depression of the static solvent permittivity by the ions, $\Delta\varepsilon_S = \varepsilon_S(c) - \varepsilon_S(0)$, to kinetic depolarisation. Hubbard, Colonomos and Wolyness (28) showed that the corrected original continuum theory yields the relationship

$$-\frac{\Delta\varepsilon_S}{\kappa} = p\,\frac{\varepsilon_S(0) - \varepsilon_\infty(0)}{\varepsilon_S(0)}\,\frac{\tau_S(0)}{\varepsilon_0} \qquad (12)$$

which predicts proportionality of the dielectric depression $\Delta\varepsilon_S$ and the specific conductance κ of the electrolyte solution. The friction factor is equal to unity for sticking, and 2/3 for slipping movement of the ions. Linearity as postulated by eq. (12) is only found at low concentrations. Fig. 3 shows the functions $\Delta\varepsilon_S$ vs.κ for solutions of $NaClO_4$ and Bu_4NClO_4 in propylene carbonate at 25°C (25). The broken lines show the limiting slopes. The solutions of NaI, Bu_4NI, $Cd(ClO_4)_2$ and $ZnBr_2$ in propylene carbonate (25), NaI, $NaClO_4$, Bu_4NI and Bu_4NClO_4 in methanol (29), and a series of 1,1, 2,1 and 2,2-electrolytes in water (19,29) are further examples studied at sufficiently low concentrations.

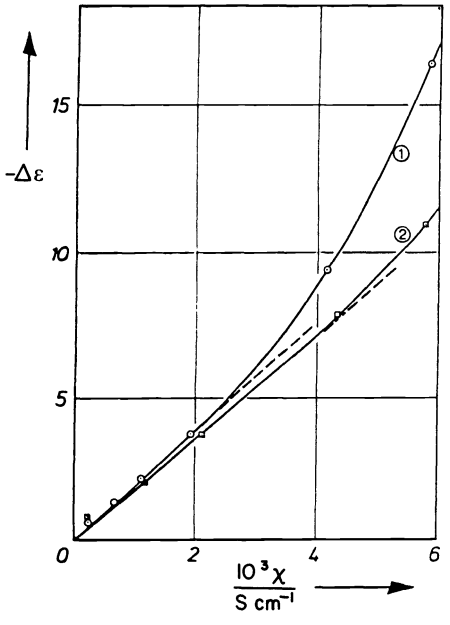

Fig. 3. Net depolarization effect of Bu_4NClO_4 (1) and $NaClO_4$ (2) solutions in propylene carbonate.

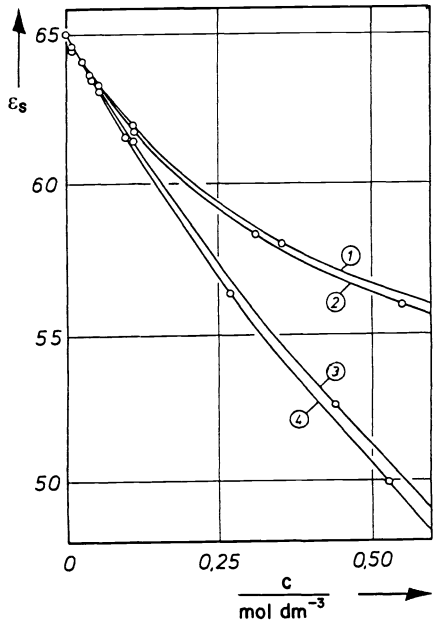

Fig. 4. Static permittivities of propylene carbonate solutions of (1) NaI; (2) $NaClO_4$; (3) Bu_4NI; (4) Bu_4NClO_4 at 25°C.

Eq. (13) links the limiting slope of function ε_S vs.c, cf. Fig. 4, to the limiting conductance Λ^∞ by the relationship

$$\lim_{c\to 0}\left(\frac{\partial\varepsilon_S}{\partial c}\right) = -p\,\frac{\varepsilon_S(0) - \varepsilon_\infty(0)}{\varepsilon_S(0)}\,\frac{\tau_S(0)}{\varepsilon_0}\,\frac{\Lambda^\infty}{10^3} \qquad (13)$$

Data analysis yields a heterogeneous pattern of results. Agreement of theory and experiment in methanol is better than in propylene carbonate or in aqueous 2,2- and 2,1-electrolyte solutions. Following Winsor and Cole (30) who assume both supersuposition of complete orientation of solvent molecules in the ionic fields as well as kinetic depolarisation, the significantly deviating experimental limiting slopes of the propylene carbonate and aqueous solutions of 2,2- and 2,1-electrolytes would require for a reduction to the theoretical slopes 3.9 (NaI), 4.4 ($NaClO_4$), 2.3 (Bu_4NI) and 2.8 (Bu_4NClO_4) orientated PC molecules and 19

($CdSO_4$), 30 ($MgSO_4$) and 18 ($MgCl_2$) water molecules, respectively. Although these numbers seem to be quite reasonable "solvation numbers" they should be accepted with some reservation due to the underlying approximations. More reliable data on dilute solutions are needed for unambiguous conclusions.

Some reliable information, however, is obtained from Fig. 4 if no heed is paid to the numerical values of solvation numbers. The sodium salts on the one hand and the tetrabutylammonium salts on the other hand exhibit that iodide and perchlorate ions should be equally solvated in propylene carbonate, in contrast to the results from IR and NMR measurements (31) which indicate no solvation for the perchlorate ion but a solvation number of 3.6 for the iodide ion.

Solvent relaxation times $\tau_s(c)$ are shifted to higher values both by alkali metal and tetraalkylammonium salt solutions in propylene carbonate (25), in contrast to methanol solutions where sodium salts decrease and tetraalkylammonium salts increase the relaxation times (2). Theory links the solvent relaxation times, $\tau_s(c)$, to the viscosity of the solution, $\eta(c)$, via microscopic relaxation times τ_s' (32). Linear functions of τ_s' vs.η are obtained for propylene carbonate solutions of Bu_4NI and Bu_4NClO_4 (25). The diameter of 0.57 nm for rotating propylene carbonate estimated from the slope of the linear function with the help of the theory of Gierer and Wirtz (33) is in good agreement with the dimensions of this molecule, d = 0.63 nm.

2.5 Temperature dependence of electrolyte conductance

A comprehensive investigation of the temperature dependence of electrolyte conductance in our laboratory shows that lithium and sodium salts in amphiprotic hydroxylic solvents require the inclusion of an OH group into the distance of closest approach of ion pairs, i.e. the lower limit a of the association integral, eq. (7a), corresponds to the configuration $C^+(OH)A^-$. Rubidium, cesium and tetraalkylammonium salts form ion pairs of type C^+A^-, potassium salts do not permit an unambiguous decision. Lithium salts are strongly solvated in electron-donor solvents and the distance of closest approach includes an orientated solvent molecule or a chelate structure, e.g. in 1,2-dimethoxyethane. Further irregularities may occur for non-symmetrical electrolytes, e.g. $CdCl_2$ behaves in methanol as a 1,1-electrolyte of type $ClCd^+Cl^-$, even at 10^{-5} M and yields ion pairs $ClCd^+(OH)Cl^-$. The 2,2-electrolytes are soluble only in water and water-rich mixtures and form the ion pairs $C^{2+}A^{2-}$, $C^{2+}(OH_2)A^{2-}$, and $C^{2+}(OH_2)_2A^{2-}$. High frequency permittivity data show that ion pairs of type $C^{2+}(OH_2)A^{2-}$ are preferred.

Table 2 shows the results of Gibbs' energies, enthalpies and entropies of ion-pair formation as obtained from such conductance measurements ($-45 \leq \vartheta/^oC \leq 25$) on ethanol solutions (12).

$$\Delta G_A = -RT \ln K_A;\ \Delta S_A = -\left(\frac{\partial \Delta G_A}{\partial T}\right)_p;\ \Delta H_A = \Delta G_A + T\Delta S_A \qquad (14a,b,c)$$

The absolute values depend on the choice of the conductance equation and the concentration scale and have no physical meaning, only their differences are significant. The non-electrostatic contributions to K_A characterized by the quantity W_{+-}^* in eq. (7a) are reflected by the non-electrostatic part of ΔG_A which is $\Delta G_A^* = N_A W_{+-}^*$.

TABLE 2. Gibbs' energy, enthalpy, and entropy of ion-pair formation in ethanol solutions at 25°C.

Electrolyte	ΔG_A	ΔH_A	ΔS_A	ΔH_A^*	ΔS_A^*
	kJ mol^{-1}	kJ mol^{-1}	J mol^{-1} K^{-1}	kJ mol^{-1}	J mol^{-1} K^{-1}
NaI	-10.24	9.73	67.0	4.03	15.5
KI	-10.76	12.42	77.7	3.00	8.3
KCNS	-10.96	11.18	74.3	4.17	16.7
CsI	-12.33	9.82	74.3	1.25	9.0
Pr_4NBr	-12.15	3.30	51.8	-2.03	1.8
Pr_4NI	-12.88	2.13	50.3	-3.04	1.2
Pr_4NClO_4	-14.09	0.75	49.8	-4.29	1.1
i-Am_3BuNI	-13.08	1.68	49.5	-3.24	1.4
$NaBPh_4$	- 9.44	5.12	48.8	0.89	3.4
i-$Am_3BuNBPh_4$	-13.77	-3.90	33.1	-7.71	-11.0

No information on the structure of ion pairs can be obtained from the ΔG_A-values and hence from the association constants K_A at 25°C. Enthalpies ΔH_A and entropies ΔS_A, however, suggest the subdivision of the data into three groups: alkali metal salts, tetraalkylammonium salts and tetraphenylborates. The tetraphenylborates exhibit about the same deficit in entropies and en-

thalpies when compared to the alkali metal or tetraalkylammonium salts with equal cations. Alkali metal and tetraalkylammonium salts differ significantly in their enthalpy and entropy values, indicating different types of ion-solvent interactions, as already illustrated by their oppositely shifting of the solvent relaxation times in alcohol solutions. Small alkali metal ions interact with the free electrons of the alcohol oxygen in contrast to the shielded charges of the large tetraalkylammonium ions (34).

Low entropies ΔS_A^* indicate that the process of ion-pair formation is accompanied by only weak rearrangement of the solvent molecules in the proximity of the respective ions. The tetraalkylammonium salts exhibit enthalpies ΔH_A^* in the order i-$Am_3BuNBPh_4$ < Pr_4NClO_4 < i-$Am_3BuNBPh_4 \approx$ Pr_4NI < Pr_4NBr, i.e. decreasing with increasing anion radii. The behaviour of alkali metal salts is more complex as a consequence of cation solvation (12). The pattern of Table 2 for ethanol solutions is also found for methanol (29) and propanol (6) solutions.

The different behaviour of tetraalkylammonium and alkali metal salts in alcohol solutions is also manifested by the functions K_A vs.T which for alkali metal salts increase continuously with temperature whereas those of tetraalkylammonium salts show significant minima. The position of the minima on the temperature axis is independent of the cation and is shifted to higher temperatures with increasing anion size (6,12) parallel to the sequence found for the enthalpies ΔH^* of ion-pair formation in Table 2.

The consistent nature of the information obtained from the chemical model is confirmed by equal heats of ion-pair formation when comparing the ΔH_A-values from temperature-dependent conductance and calorimetric measurements of heat of dilution (2,7,35).

2.6 Conductance of low permittivity solutions

Electron donor solvents of low permittivity such as diethylether, tetrahydrofuran or 1,2-dimethoxyethane and inert solvents such as trichloroethylene or benzene as well as their mixtures with aprotic solvents are of increasing interest in modern technologies. Ethers exhibit exceptionally high solubilities for various electrolytes and are frequently used as components of mixed solvent systems. Solvents of low permittivity show particular transport properties, some of which are attributed to triple-ion formation of the electrolytes in these solvents.

The dependence of conductance on concentration and temperature of $LiBF_4$ solutions in 1,2-dimethoxyethane from infinite dilution to saturation is shown in Fig. 5a by the conductance functions at 25°C and -45°C (36). The plots of Λ vs.$\sqrt{c}$ show minima at moderate and maxima at high concentrations as a consequence of the competition of free ions, ion pairs, triple ions and higher ion aggregates. Intersection of the two curves occurs at 0.4 M. A second point of intersection at concentrations below 10^{-5} M cannot be attained by measurements but follows clearly from the comparison of the extrapolated values of Λ^∞ in Table 3. As a consequence, a region of very low concentrations showing a positive temperature coefficient of conductance is followed by a region with a negative temperature coefficient, cf. Fig. 5b, and this in turn by a region in which the temperature coefficient is again positive.

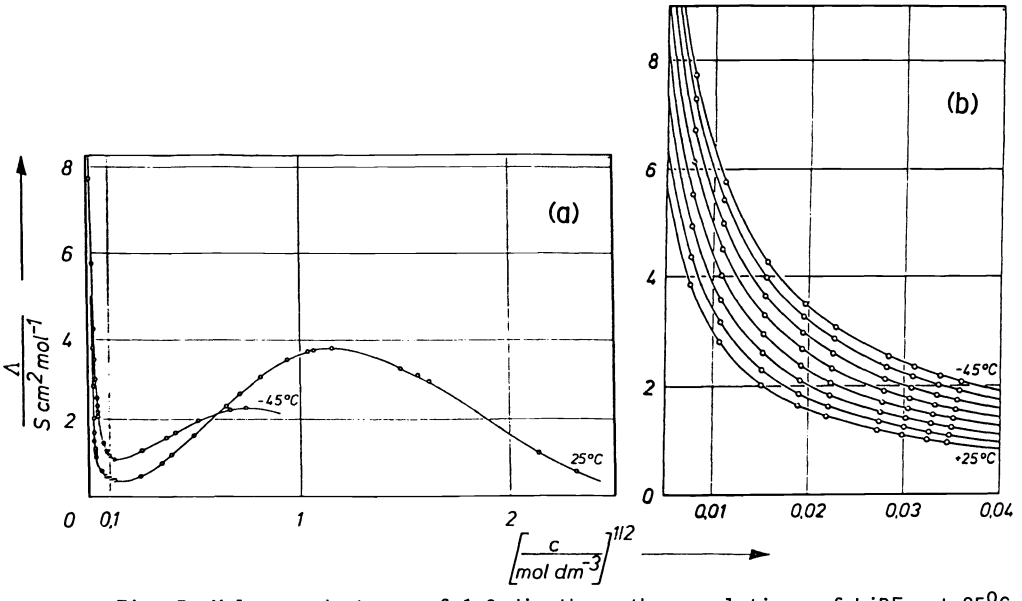

Fig. 5. Molar conductance of 1,2-dimethoxyethane solutions of $LiBF_4$ at 25°C and -45°C.
(a) from infinite dilution to saturation; (b) at moderate concentrations (steps of 10°C)

Extrapolation to Λ^∞ from concentrations distinctly below the conductance minimum may neglect the role of triple ions. Table 3, first line, compiles the values of Λ^∞ as obtained by a fit according to eq. (8b). The most reliable value of Λ^∞ is obviously that which is obtained at -45°C where the measured values attain about 20 % of Λ^∞. The extrapolations at higher temperatures are increasingly affected by systematic errors due to the distances between measured values Λ and Λ^∞, e.g. $\Lambda/\Lambda^\infty < 0.03$ at 25°C. A reliable estimation of Λ^∞ at higher temperatures can be based, however, on eq. (11) supposing the value of Λ^∞ at -45°C to be correct, cf. Table 3, second line.

TABLE 3. Limiting conductance and association constants of ion-pair and triple-ion formation for $LiBF_4$ solutions in 1,2-dimethoxyethane at various temperatures.

Temp. eq.	$\Theta/^oC$	-45	-35	-25	-15	-5	+5	+15	+25
(8b)	$\Lambda^\infty/Scm^2mol^{-1}$	46.5	55.7	65.3	74.1	80.5	86.4	84.0	76.1
(11)	$\Lambda^\infty/Scm^2mol^{-1}$	(46.5)	57.2	68.8	81.1	94.1	108.1	123.1	139.3
(15)	$10^{-6}K_A/mol^{-1}dm^3$	0.53	1.0	1.7	3.0	5.0	8.4	13.9	22.9
	$K_T/mol^{-1}dm^3$	14.9	17.0	18.9	21.0	23.1	25.4	28.0	30.8

The conductance equation of Fuoss and Kraus (37)

$$\frac{\Lambda y_\pm' \sqrt{c}}{1 - S(\Lambda^\infty)^{-3/2}\sqrt{\Lambda c(1-\Lambda/\Lambda^\infty)}} = \frac{\Lambda^\infty}{\sqrt{K_A}} + \lambda_T^\infty \frac{K_T}{\sqrt{K_A}}\left(1 - \frac{\Lambda}{\Lambda^\infty}\right)c \qquad (15)$$

is the appropriate equation for reproducing the conductance curve up to concentrations near to the conductance minimum. In eq. (15) $y_\pm'$ is the mean activity coefficient of the free ions, S is the limiting slope of eq. (8b), λ_T^∞ is the hypothetical limiting value of the tripe ions $[C^+A^-C^+]^+$ and $[A^-C^+A^-]^-$, K_A and K_T are the equilibrium constants of ion-pair and triple-ion formation

$$C^+ + A^- \overset{K_A}{\rightleftarrows} [C^+A^-]; \quad A^- + [C^+A^-] \overset{K_T}{\rightleftarrows} [A^-C^+A^-]^-; \quad C^+ + [A^-C^+] \overset{K_T}{\rightleftarrows} [C^+A^-C^+]^+$$

Table 3, lines 3 and 4 report the values of K_A and K_T obtained by data analysis based on eq. (15) when λ_T^∞ is set to $2\Lambda^\infty/3$ (36,38). Both ion-pair and triple-ion formation decrease with decreasing temperature in accordance with increasing solvent permittivities. Triple-ion formation is rather poor and would be negligible at permittivities of about 15 [ε(DME, -45°C) = 10.1, m.p. (DME) = -58°C]. Using the asymptotic approximation for triple-ion formation (39) and the values of K_T from Table 3 the contact distance, a_3, in the triple ions is found to be 0.32 (-45°C) < a_3/nm < 0.27 (+25°C) in good agreement with the ionic radii, $a_+(Li^+)$ = 0.078 nm and $a_-(BF_4^-)$ = 0.232 nm. Ion-pair formation entails a significant change in entropy, ΔS_A, due to the rearrangement of the solvent molecules around the strongly solvated Li^+ ion in the electron donor solvent, 1,2-dimethoxyethane.

3. ELECTROLYTES AT HIGH CONCENTRATIONS

Three classes of empirical transport equations can be found in the literature: molten salt approaches, extensions of the equations for dilute solutions, and empirical equations for fitting the measured data (2). Equations based on ion distribution functions are not available.

The fused salt approach of Vogel, Fulcher, and Tamann, when based on the equilibrium distribution of an isothermal, isobaric ensemble of the cooperatively rearranging domains in a liquid considers the ideal glass transition temperature T^o to be the appropriate reference temperature for transport and relaxation processes in the liquid state, cf. ref. (40,41) and quoted literature. The Vogel-Fulcher-Tamann (VFT) equation has been repeatedly used in the form

$$W(T) = A(T) \exp\left[-\frac{B}{T-T^o}\right] \qquad (16)$$

for analyzing the temperature dependence of various transport properties W(T) and for determining the ideal glass transition temperature T^o by appropriate extrapolation methods. The pre-exponential factor A(T) can be used in various forms, A(T) = A'f(T) (41,42). Angell (43) and Spiro and King (41) stress that the temperature dependence of A(T) is of minor importance and can be omitted if $T/T^o < 2$ (43) or if W(T) is any property other than diffusion (41). We have used eq. (16) for investigating transport properties of non-aqueous electrolyte solutions and their solvents on the basis of Angell's concept (44).

3.1 Specific conductance

The conductance of concentrated electrolyte solutions and its temperature dependence are of crucial interest for high energy and low temperature batteries, plating baths, electrolysis etc. Only a few sets of comprehensive data which are suitable for the discussion of conductance-determining effects are available (14) and show remarkable deviations, e.g. the specific conductance of 1 M $LiClO_4$ solutions in propylene carbonate is found to be (45) 5.6×10^{-3}, 4.36×10^{-3}, or 3.9×10^{-3} S cm^{-1}.

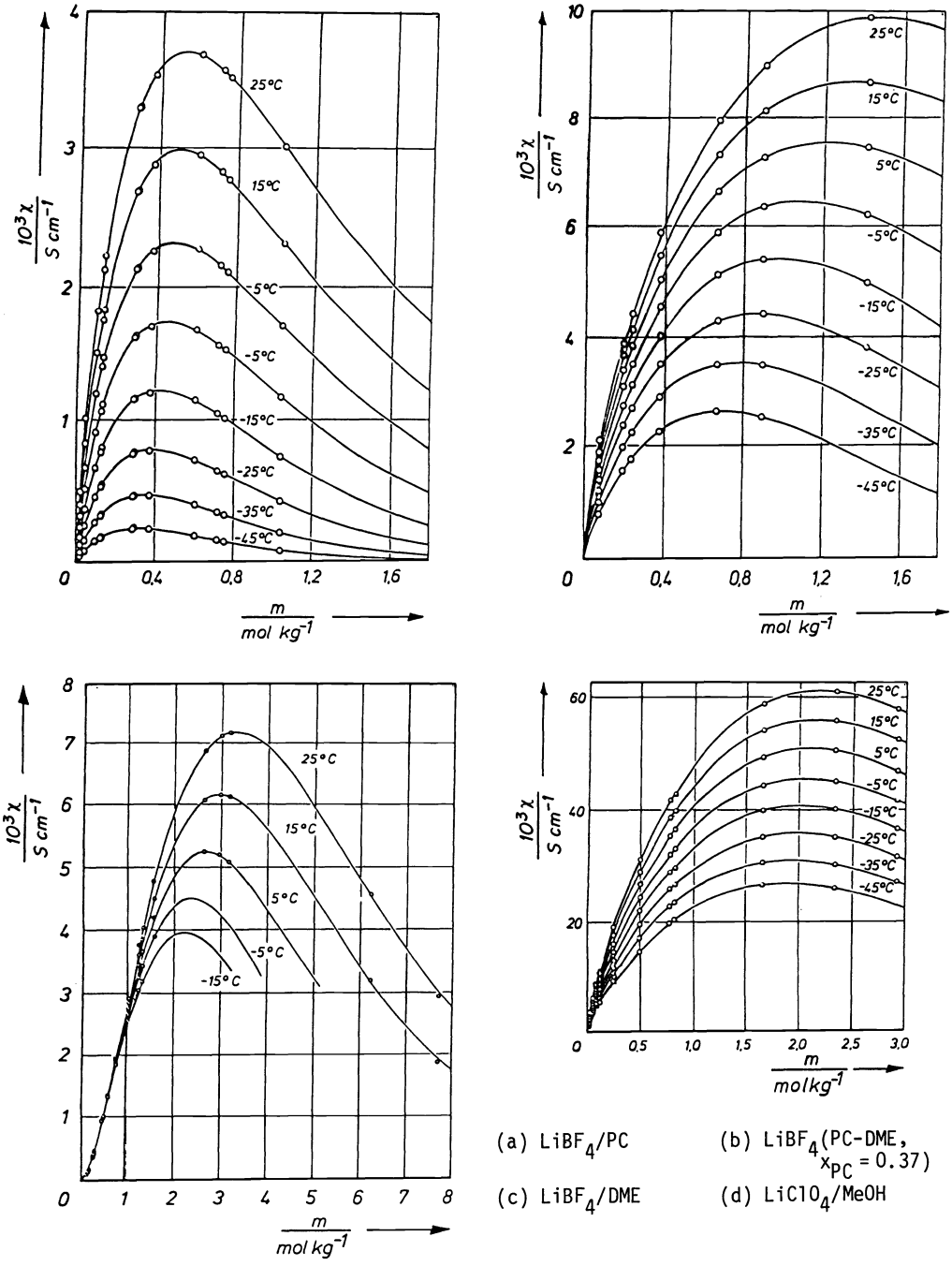

Fig. 6. Diagrams κ-m-T for various electrolyte solutions.
κ(specific conductance), m(molality), T(temperature)

Figs. 6 show the features of specific conductance in a protic (MeOH), aprotic (PC), low permittivity electron donor solvent (DME), and in a solvent mixture (PC-DME). In spite of permittivities varying from 65 (PC at 25°C) to 7.1 (DME at 25°C) and distinctly different asso-

ciation constants in the PC-DME solvent mixtures the maxima of specific conductance exhibit the same order of magnitude, low permittivity solutions at high concentrations being even better conductors than the solutions of the same electrolyte in solvents of high permittivities (45,46). The negative temperature coefficient of the $LiBF_4$/DME system at moderate concentrations, Fig. 5, is reflected by almost temperature-independent specific conductances up to 0.4 M, Fig. 6a; above 0.4 M the curves fan out and attain their maxima in the usual way. This technologically interesting behaviour is also observed for DME-rich solvent mixtures. The maximum of methanol (ε = 34 at 25°C) solutions is found at higher conductances and higher concentrations when compared to the propylene carbonate solutions.

The maximum of specific conductance κ_{max} and its interpretation is one of the main interests of investigations into concentrated solutions (45-49). The variation of specific conductance is related to the molar conductance, Λ, and the molar density function, ρ, of the electrolyte compound by

$$d\kappa = \Lambda d\rho + \rho d\Lambda \qquad (17)$$

Discussion is limited to the concentration region of maximum specific conductance where $d\Lambda < 0$ if $d\rho > 0$, also for solvents such as 1,2-dimethoxyethane. The maximum of specific conductance, $d\kappa = 0$, follows from the competition between the increase $d\rho$ of the ionic density and the lowering $d\Lambda$ of the ionic mobility when the electrolyte concentration increases. The analysis of κ-m-T diagrams, Figs. 6, for various electrolytes in propylene carbonate and methanol solutions yields the result shown in Figs. 7: The maximum of specific conductance κ_{max} and the concentration μ at which it is attained are correlated. This indicates the existence of an energy barrier to conductance which appears to depend solely on solvent properties, particularly on viscosity. At concentration μ corresponding to the maximum κ_{max} in the κ(m) curve the electrolyte shows an activation energy of the transport process equivalent to that of the barrier (46). Electrolyte solutions in methanol can be divided into the same classes already referred to in the discussion of the short-range potentials in dilute solutions, cf. section 2.5. In propylene carbonate no such division is apparent, the sequence depending rather on the ionic Stokes' radii (45).

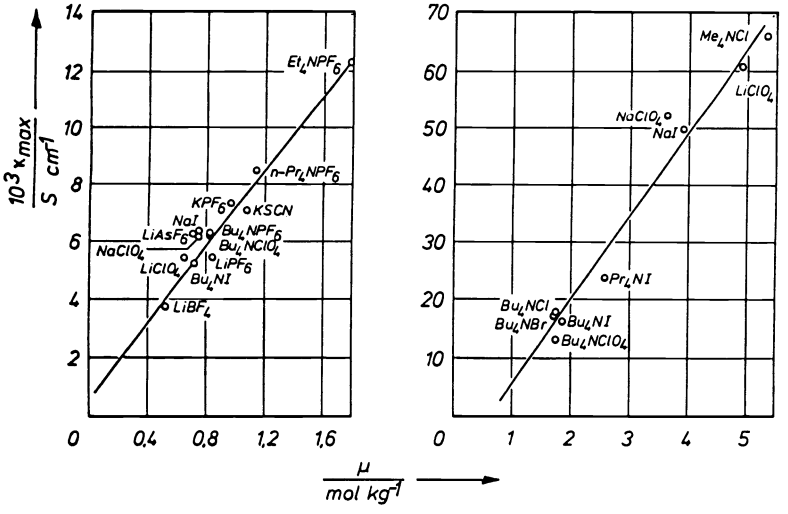

Fig. 7. Dependence κ_{max} vs.μ for various salts in (a) propylene carbonate and (b) methanol at 25°C.

Organic solvent mixtures exhibit the same features. The complete κ-m-T-ξ diagrams are known for some electrolytes in propylene carbonate-dimethoxyethane mixtures in the temperature range from -45 to 25°C, solvent composition ξ varying from zero to 100 % of weight (45,46). The concentration μ at maximum specific conductance decreases with decreasing temperature for every solvent composition, i.e. with increasing viscosity. An increase of viscosity at constant temperature resulting from a change in solvent composition produces a decrease in μ, also proving that viscosity is here the most important conductance determining factor. The states of PC-DME solutions at infinite dilution and at maximum conductance are corresponding states in terms of the temperature coefficient of the charge transport process, i.e. the maximum specific conductance is attained when the conductance determining effects have established the critical energy barrier imposed by the solvent. The state at infinite dilution is discussed in section 3.2. The linear correlation κ_{max} vs.μ is observed for all mixtures and at

all temperatures. In spite of large ion-ion association constants, e.g. DME and DME-rich mixtures, unexpectedly high κ_{max}-values can be found when the corresponding μ-values are large.

The knowledge of complete κ-m-T or κ-m-T-ξ diagrams permits the rationalization of some properties of concentrated solutions in terms of the parameters which characterize the dilute solutions (45,46), e.g. comparison of a mobility function $(\kappa/m)_\xi$ for various electrolytes indicates a change in the Li^+ ion solvation with increasing DME content of DME-PC mixtures, in contrast to K^+ and Et_4N^+ ions and the role of association constants (46). Solvation of Li^+ ions by DME in these solvents has been confirmed meanwhile also by other methods (50).

3.2 Glass transition temperature and transport properties

Propylene carbonate solutions are suitable candidates for applying the VFT equation to non-aqueous solutions because of their high permittivities restricting ion-pair formation to a small extent and their high temperature coefficients of viscosity. The glass transition temperature of the solution at molality m, $T^o(m)$, is assumed to be

$$T^o(m) = T^o(0) + am + bm^2;\ T^o(0) = \lim_{m\to 0} T^o(m) \qquad (18a,b)$$

The temperature dependence of specific conductance at molality m, $\kappa_m(T)$, is then given by the relationship

$$\kappa_m(T) = A_m^{(\kappa)} \exp\left[-\frac{B_m^{(\kappa)}}{R(T-T^o(m))}\right] \qquad (19)$$

In eq. (19) $A_m^{(\kappa)}$ and $B_m^{(\kappa)}$ are temperature independent functions of molality m, R is the gas constant.

Conductance theory requires

$$\lim_{m\to 0} \frac{\kappa_m(T)}{m} = \Lambda^{\infty(m)}(T);\ \text{i.e. } A_m^{(\kappa)} = \alpha m + \text{higher terms} \qquad (20)$$

Data analysis confirms the form of $A_m^{(\kappa)}$ required by eq. (20).

A similar equation is obtained for the fluidity, $\phi = \eta^{-1}$, of the solvent.

$$\phi(T) = A^{(\phi)} \exp\left[-\frac{B^{(\phi)}}{R(T-T^o)}\right];\ B^{(\phi)} = -B^{(\eta)};\ A^{(\phi)} = \frac{1}{A^{(\eta)}} \qquad (21)$$

The coefficients of eq. (18a) obtained from data analysis for 14 electrolytes in propylene carbonate (45) are given in Table 4.

TABLE 4. Parameters of eq. (19) for various salts in propylene carbonate.

Electrolyte	$T^o \pm \sigma(T^o(0))$ / K	$a \pm \sigma(a)$ / K kg mol^{-1}	$b \pm \sigma(b)$ / K kg^{2}mol^{-2}	σ_{fit} / K
$LiBF_4$	151.58 ± 0.41	26.6 ± 3.3	-16.2 ± 4.1	0.60
$LiClO_4$	152.58 ± 0.45	25.2 ± 1.3	- 5.7 ± 0.8	0.20
$LiPF_6$	149.61 ± 0.33	20.8 ± 1.6	- 5.2 ± 1.6	0.22
$LiAsF_6$	151.16 ± 0.10	19.4 ± 0.5	- 1.5 ± 0.5	0.12
NaI	151.52 ± 0.39	38.5 ± 2.0	-12.7 ± 1.9	0.39
$NaClO_4$	153.04 ± 0.28	22.4 ± 0.9	- 3.7 ± 0.5	0.15
KPF_6	152.22 ± 0.22	25.2 ± 1.0	-10.4 ± 0.9	0.16
KCNS	150.81 ± 0.11	12.9 ± 0.3	- 0.6 ± 0.2	0.06
Et_4NPF_6	152.09 ± 0.13	9.28 ± 0.4	- 2.4 ± 0.3	0.06
Pr_4NPF_6	151.96 ± 0.21	7.96 ± 1.2	1.6 ± 1.1	0.10
Bu_4NI	150.96 ± 0.10	9.10 ± 0.6	- 3.5 ± 0.6	0.12
Bu_4NPF_6	151.43 ± 0.23	6.49 ± 0.8	0.2 ± 0.5	0.22
Bu_4NClO_4	151.34 ± 0.28	6.75 ± 0.7	- 1.5 ± 0.3	0.31

The individual $\sigma(T^o(0))$-values in Table 4 do not take into account the uncertainty of the $T^o(m)$-values which, however, can be estimated from the relevant 95 % confidence intervals. For example, the confidence interval for $LiBF_4$/PC at the lowest concentration measured, m = 0.018 mol kg^{-1}, is found to be 4.82 K, yielding a $T^o(m)$-value in the range of 149.37 to 154.19 K. The mean value from all solutions of Table 4 is $T^o(0)$ = (151.56 ± 0.87)K. The slopes at m = 0 of the curves $T^o(m)$ vs.m, eq. (18a), are found to be in the order of the re-

ciprocal ionic radii, in agreement with Angell's observation for mixed-salt melts (51).

The determination of T^o from three independent series of measurements of the temperature dependence of viscosity yields a mean value of T^o = (152.11 ± 0.69)K, the confidence interval for a single series of viscosity measurements ranging from 149.9 to 154.3 K. The good agreement of results from both conductance and viscosity measurements permits the estimate of T^o = 152 K as the ideal glass transition point of propylene carbonate.

The temperature dependences of specific conductance and fluidity are given by the relationships

$$-R\,\frac{d\ln\kappa_m}{d(1/T)} = E^{(m)}(m,T) = B_m^{(\kappa)}\,\frac{T^2}{(T-T^o(m))^2};\quad -R\,\frac{d\ln\phi}{d(1/T)} = E^{(\eta)} = -B^{(\eta)}\,\frac{T^2}{(T-T^o)^2} \qquad (22a,b)$$

Data analysis yields equal $B_0^{(\kappa)}$-values for all electrolytes in Table 4 independent of the shape of the curves of $B_m^{(\kappa)}$ vs.m, thus confirming the infinite dilution to be a corresponding state in terms of activation energy of conductance. Again $B_0^{(\kappa)}$ equals $B^{(\eta)}$ obtained from viscosity.

$$\lim_{m\to 0} B_m^{(\kappa)} = B_0^{(\kappa)} = (3350 \pm 50)\ \mathrm{J\ mol^{-1}};\quad B^{(\eta)} = -(3420 \pm 50)\ \mathrm{J\ mol^{-1}} \qquad (23a,b)$$

From eqs. (22) and (23) it follows that the activation energies of conductance at infinite dilution and viscosity are equal at every temperature.

The activation energies at infinite dilution, as obtained from concentrated solutions with the help of the model of cooperatively rearranging domains, agree well with those estimated from conductance measurements on dilute solutions by means of MMF-level models, after conversion of the concentration scales. Table 5 summarizes the results.

TABLE 5. Comparison of activation energies of conductance of various salts in propylene carbonate.

Temp.	Extrapolation from concentrated solutions		Extrapolation from dilute solutions	
Θ / °C	$E^{(\kappa)}(0,T)$ / kJ mol^{-1}	$E^{(\Lambda)}(0,T)$ / kJ mol^{-1}	$E^{(\Lambda)}(0,T)$ / kJ mol^{-1}	
	14 electrolyte solutions		KPF_6	$LiClO_4$
25	13.9	14.5	14.5	14.3
15	14.9	15.5	15.5	15.3
5	16.2	16.7	16.7	16.6
- 5	17.7	18.2	18.2	18.0
-15	19.7	20.2	20.1	19.9
-25	22.1	22.6	22.4	22.2
-35	25.4	25.7	25.5	25.2

The infinitely dilute solution is also confirmed as a corresponding state of the activation energy of transport from investigations on dilute solutions with the aid of the chemical model for the solvents methanol (29), ethanol (see section 2.3), propanol (6), and acetronitrile (6).

REFERENCES

1. H.-J. Gores and J. Barthel, Naturwissenschaften, 70, 495 - 503 (1983).
2. J. Barthel, H.-J. Gores, G. Schmeer, and R. Wachter, Topics in Current Chemistry, Ed. by F. L. Boschke, Springer, Heidelberg, 111, 33 - 144 (1983).
3. Parameters and literature quoted in ref. 2.
4. H. L. Friedman, Faraday Discuss. Chem. Soc., 64, 7 - 15 (1977).
5. J. Barthel, Ber. Bunsenges. Phys. Chem., 83, 252 - 257 (1979).
6. J. Barthel, Pure Appl. Chem., 51, 2093 - 2124 (1979).
7. J. Barthel, Proceedings of the 9th International CODATA Conference, Ed. by P. Glaeser, North Holland, Amsterdam (1984) (in press).
8. M. Spiro, Physical Chemistry of Organic Solvent Systems, Ed. by A. K. Covington and T. Dickinson, Plenum Press, London, 615 - 680 (1973).
9. J. Periê, M. Periê, and J.-C. Justice, J. Solution Chem. 9, 395 - 414 (1980).
10. J.-C. Justice, J. Periê, and M. Periê, J. Solution Chem. 9, 583 - 605 (1980).
11. J. Barthel, U. Ströder, L. Iberl, and H. Hammer, Ber. Bunsenges. Phys. Chem., 86, 636 -

645 (1982).
12. J. Barthel, R. Neueder, F. Feuerlein, F. Straßer, and L. Iberl, J. Solution Chem. 12, 449 - 471 (1983).
13. B. S. Krumgalz, J. Chem. Soc. Faraday Trans. 1, 79, 571 - 587 (1983).
14. J. Barthel, R. Wachter, and H.-J. Gores, Modern Aspects of Electrochemistry, Ed. by B. E. Conway and J. O'M. Bockris, Plenum Publ. Corp., New York, 13, 1 - 79 (1979).
15. J.-C. Justice, Comprehensive Treatise of Electrochemistry, Ed. by B. E. Conway, J. O'M. Bockris, and E. Yeager, Plenum Press, New York 5, 223 - 338 (1983).
16. A. R. Altenberger and H. L. Friedman, J. Chem. Phys., 78, II, 4162 - 4173 (1983).
17. A. D. Pethybridge, Z. Phys. Chem. N. F., 133, 143 - 158 (1982).
18. J.-C. Justice and J. Barthel, Techniques de l'Ingénieur (in press).
19. J. Barthel, R. Buchner, and H.-J. Wittmann, Z. Phys. Chem. N. F. (in press).
20. R. L. Kay and J. L. Dye, Proc. Natl. Acad. Sci, 49, 5 - 11 (1963).
21. G. A. Vidulich, G. P. Cunningham, and R. L. Kay, J. Solution Chem. 2, 23 - 35 (1973).
22. R. Pottel, Ber. Bunsenges. Phys. Chem., 69, 363 - 378 (1965).
23. J.-C. Lestrade, J.-P. Badiali, and H. Cachet, Dielectric and Related Molecular Processes, Ed. by M. Davies, The Chemical Soc. London, 2, 106 - 150 (1975).
24. J. Barthel, H. Behret, and F. Schmithals, Ber. Bunsenges. Phys. Chem., 75, 305 - 309 (1971).
25. J. Barthel and F. Feuerlein, J. Solution Chem. 13, 393 - 417 (1984).
26. J. B. Hubbard and L. Onsager, J. Chem. Phys., 67, 4850 - 4857 (1977).
27. J. B. Hubbard, J. Chem. Phys. 68, 1649 - 1664 (1978).
28. J. B. Hubbard, P. Colonomos, and P. G. Wolynes, J. Chem. Phys. 71, 2652 - 2661 (1979).
29. data from our laboratory (to be published).
30. P. Winsor, IV, and R. H. Cole, J. Phys. Chem. 86, 2491 - 2494 (1982).
31. H. L. Yeager, J. D. Fedyk, and R. J. Parker, J. Phys. Chem. 77, 2407 - 2410 (1973).
32. N. E. Hill, W. E. Vaughan, A. H. Price, and M. Davies, Dielectric Properties and Molecular Behaviour, Van Nostrand Reinhold Co., London (1969).
33. A. Gierer and K. Wirtz, Z. Naturf., 8a, 532 - 538 (1953).
34. J. Barthel, H.-J. Wittmann, and M. Krell (in preparation).
35. R. Wachter and K. Riederer, Pure Appl. Chem., 53, 1301 - 1312 (1981).
36. J. Barthel, R. Gerber, and H.-J. Gores, Ber. Bunsenges. Phys. Chem. (in press).
37. R. M. Fuoss and C. A. Kraus, J. Am. Chem. Soc., 55, 2387 - 2399 (1933).
38. S. Boileau and P. Hemery, Electrochim. Acta, 21, 647 - 655 (1976).
39. R. M. Fuoss, J. Am. Chem. Soc., 56, 1857 - 1859 (1934).
40. S. I. Smedley, The Interperetation of Ionic Conductivity in Liquids, Plenum Press, New York (1980).
41. M. Spiro and F. King, Ionic Liquids, Ed. by D. Inman and D. G. Lovering, Plenum Press, London, 57 - 77 (1981).
42. J. Melsheimer and K. Langner, Ber. Bunsenges. Phys. Chem., 83, 539 - 544 (1979).
43. C. A. Angell, Aust. J. Chem. 23, 929 - 937 (1970).
44. J. Barthel, H.-J. Gores, P. Carlier, F. Feuerlein, and M. Utz, Ber. Bunsenges. Phys. Chem. 87, 436 - 443 (1983).
45. J. Barthel, H.-J. Gores, and G. Schmeer, Ber. Bunsenges. Phys. Chem. 83, 911 - 920 (1979).
46. H.-J. Gores and J. Barthel, J. Solution Chem., 9, 939 - 954 (1980).
47. J. Molenat, J. Chim. Phys. 66, 825 - 832 (1969).
48. V. M. Valyashko and A. A. Ivanov, Zh. Neorg. Khim., 19, 2978 - 2983 (1974).
49. R. Jasinski, Advances in Electrochemistry and Electrochemical Engineering, Ed. by P. Delahay and Ch. W. Tobias, Wiley, New York, 8, 253 - 335 (1971).
50. Y. Matsuda, H. Nakashima, M. Morita, and Y. Takasu, J. Electrochem. Soc., 2552 - 2556 (1981).
51. C. A. Angell, J. Phys. Chem., 68, 1917 - 1929 (1964).